The Journal of Immunology

A Comparative Analysis of Multiple Sclerosis–Relevant Anti-Inflammatory Properties of Ethyl Pyruvate and Dimethyl Fumarate

Djordje Miljkovic, Jana Blazevski, Filip Petkovic, Neda Djedovic, Miljana Momcilovic, Suzana Stanisavljevic, Bojan Jevtic, Marija Mostarica Stojkovic and Ivan Spasojevic

J Immunol published online 13 February 2015
http://www.jimmunol.org/content/early/2015/02/13/jimmunol.1402302

The Journal of Immunology is published twice each month by The American Association of Immunologists, Inc., 9650 Rockville Pike, Bethesda, MD 20814-3994.

Print ISSN: 0022-1767 Online ISSN: 1550-6606.

Published February 13, 2015, doi:10.4049/jimmunol.1402302

A Comparative Analysis of Multiple Sclerosis–Relevant Anti-Inflammatory Properties of Ethyl Pyruvate and Dimethyl Fumarate

Djordje Miljković,* Jana Blaževski,* Filip Petković,* Neda Djedović,* Miljana Momčilović,* Suzana Stanisavljević,* Bojan Jevtić,* Marija Mostarica Stojković,† and Ivan Spasojević‡

Dimethyl fumarate (DMF), a new drug for multiple sclerosis (MS) treatment, acts against neuroinflammation via mechanisms that are triggered by adduct formation with thiol redox switches. Ethyl pyruvate (EP), an off-the-shelf agent, appears to be a redox analog of DMF, but its immunomodulatory properties have not been put into the context of MS therapy. In this article, we examined and compared the effects of EP and DMF on MS-relevant activity/functions of T cells, macrophages, microglia, and astrocytes. EP efficiently suppressed the release of MS signature cytokines, IFN-γ and IL-17, from human PBMCs. Furthermore, the production of these cytokines was notably decreased in encephalitogenic T cells after in vivo application of EP to rats. Production of two other proinflammatory cytokines, IL-6 and TNF, and NO was suppressed by EP in macrophages and microglia. Reactive oxygen species production in macrophages, microglia activation, and the development of Ag-presenting phenotype in microglia and macrophages were constrained by EP. The release of IL-6 was reduced in astrocytes. Finally, EP inhibited the activation of transcription factor NF-κB in microglia and astrocytes. Most of these effects were also found for DMF, implying that EP and DMF share common targets and mechanisms of action. Importantly, EP had in vivo impact on experimental autoimmune encephalomyelitis, an animal model of MS. Treatment with EP resulted in delay and shortening of the first relapse, and lower clinical scores, whereas the second attack was annihilated. Further studies on the possibility to use EP as an MS therapeutic are warranted. ***The Journal of Immunology*****, 2015, 194: 000–000.**

The pathophysiology of multiple sclerosis (MS) involves two main components: inflammatory and neurodegenerative. Both of them are apparently tackled by dimethyl fumarate (DMF; BG-12, Tecfidera), a drug that has been recently approved in the United States, Australia, Canada, and the European Union as a first-line treatment for patients suffering from relapsing forms of MS. Namely, DMF induces apoptosis of Th cells, shifts Th balance toward nonpathogenic Th2 phenotype, inhibits differentiation of APCs, reduces release of proinflammatory cytokines from glial cells, and downregulates expression of adhesion molecules on endothelial cells, thus interfering with leukocyte migration (1). In addition, DMF protects neurons and astrocytes from inflammation- and neurodegeneration-related oxidative stress by activating the endogenous defense system and blocking pro-oxidative cascades (2). The activity of DMF appears to be prevalently based on redox properties, that is, binding to thiols via Michael-type addition (3). DMF turns off thiol redox switches on T cell membrane, whereas in neurons and astrocytes, DMF targets specific thiol moieties, which leads to activation of Nrf2-controled set of antioxidative enzymes, NAD(P)H: quinine oxidoreductase 1 and glutathione-related enzymes, and downregulation of transcription factor NF-κB (2, 4, 5). These pharmacological strategies—targeting of redox switches to suppress T cell activity (6–8), and activation of endogenous antioxidative system instead of frequently futile application of exogenous antioxidants (9)—are rather new and hold promise of further therapeutic relevance.

We have noted recently that ethyl pyruvate (EP) might represent a DMF redox analog, and therefore could be of interest in MS treatment (5). EP forms Michael-type adducts with thiols, activates Nrf2 in astrocytes, and inhibits NF-κB–dependent transcription in different cell types, including LPS-stimulated BV2 (microglial) cells and macrophage-like RAW 264.7 cells (10–13). Anti-inflammatory and neuroprotective effects of EP have been observed in animal models of sepsis, uveitis, and asthma (14–16). EP has been effective also against different neurologic insults, such as ischemia/reperfusion (17), intracerebral hemorrhage-induced brain injury (18), traumatic brain injury (19), 1-methyl-4-phenyl-1,2,3,6-tetrahydropyridine (20), LPS (21), and 3-nitropropionic acid (22). Still, potential immunomodulatory effects of EP that are of relevance for MS pathology and therapy have not been examined so far.

Immune cells, as well as CNS resident cells, are important players in the pathogenesis of MS and its animal model: experimental autoimmune encephalomyelitis (EAE). This model has been proved useful in studying pathological mechanisms of MS. Also, some of the MS therapies, including Copaxone and natalizumab, emerged from EAE studies (23). Th phenotypes that produce IFN-γ or IL-17, that is, Th1

*Department of Immunology, Institute for Biological Research "Siniša Stanković," University of Belgrade, 11000 Belgrade, Serbia; †Institute of Microbiology and Immunology, School of Medicine, University of Belgrade, 11000 Belgrade, Serbia; and ‡Life Sciences Department, Institute for Multidisciplinary Research, University of Belgrade, 11030 Belgrade, Serbia

Received for publication September 8, 2014. Accepted for publication January 15, 2015.

This work was supported by Ministry of Education, Science and Technological Development of the Republic of Serbia Grants OI173035, OI175038, OI173014, and OI173013.

Address correspondence and reprint requests to Dr. Djordje Miljković, Institute for Biological Research "Siniša Stanković," Department of Immunology, Bulevar Despota Stefana 142, 11000 Belgrade, Serbia. E-mail address: djordjem@ibiss.bg.ac.rs

Abbreviations used in this article: BMDM, bone marrow–derived macrophage; c.s., clinical sign; DEPMPO, 5-diethoxyphosphoryl-5-methyl-1-pyrroline-*N*-oxide; DLNC, draining lymph node cell; DMF, dimethyl fumarate; EAE, experimental autoimmune encephalomyelitis; EP, ethyl pyruvate; EPR, electron paramagnetic resonance; GSH, reduced glutathione; iNOS, inducible NO synthase; MS, multiple sclerosis; PM, peritoneal macrophage; PPD, purified protein derivative; ROS, reactive oxygen species; SCH, spinal cord homogenate; SCIC, spinal cord immune cell; TT, tetanus toxoid.

and Th17 cells, are considered to be the major pathogenic population in MS and EAE (24). Their interactions with APCs, such as dendritic cells and macrophages, both within the CNS and in lymphoid organs, are essential for initiation and propagation of autoimmune response directed against the CNS (25). Deregulated macrophages and microglia largely contribute to CNS tissue destruction via generation of proinflammatory cytokines, NO, and reactive oxygen species (ROS) (26). Moreover, microglia and even astrocytes might be important for the process of Ag presentation within the CNS (25). Beyond this possibility, both microglia and astrocytes appear to contribute to injury, but also to the protection and repair of CNS tissue during pathogenesis of MS and EAE (27, 28). Thus, the modulation of immune activity of these cells represents an important therapeutic target in MS treatment.

The aim of this study was to compare the effects of EP and DMF on various functions of cells that contribute to MS pathogenesis: T cells, macrophages, microglia, and astrocytes. We examined a battery of MS-relevant parameters: the production of proinflammatory cytokines (IFN-γ, IL-17, IL-6, and TNF), generation of NO and ROS, expression of Ag presentation–related molecules, and phagocytosis. It appears that EP and DMF affected the examined parameters in a similar manner. Finally, effects of EP on EAE in rats were examined showing that this agent alleviates the disease.

Material and Methods

Experimental animals and EAE induction

Dark Agouti rats (female, 2–4 mo old) were used in this study. The rats were maintained in the animal facility of the Institute for Biological Research "Siniša Stanković." Animal manipulation and experimental procedures were approved by the local Ethics Committee (Institute for Biological Research "Siniša Stanković", no. 2-10/13). EAE was induced with rat spinal cord homogenate (SCH) in PBS (50% w/v) mixed with equal volume of CFA (Difco, Detroit, MI) and supplemented with *Mycobacterium tuberculosis* (to 5 mg/ml). Animals were injected as described previously (29). Animals were monitored daily for EAE clinical signs (c.s.) and scored according to the following scale: 0 = no c.s.; 1 = flaccid tail; 2 = hind-limb paresis; 3 = hind-limb paralysis; 4 = moribund state or death. Cumulative c.s. was calculated as the sum of daily clinical scores, whereas average c.s. was calculated as cumulative c.s. divided by the number of days with clinically manifested EAE. Rats were treated i.p. with EP (300 mg/kg body weight; Sigma-Aldrich, St. Louis, MO) or vehicle (PBS), once per day, starting from day 8 postimmunization.

Isolation of cells and cell cultures

Human PBMCs were isolated from fresh blood samples of healthy volunteers (individuals who have been vaccinated with BCG vaccine and against tetanus). All procedures related to the use of human blood are in conformity with the recommendation provided in the Code of Ethics of the World Medical Association (Declaration of Helsinki). PBMCs were purified by centrifugation on Histopaque 1077 (Sigma-Aldrich), according to the manufacturer's instructions. The cells were seeded at 1×10^6/ml in 24-well plates (Sarstedt, Nümbrecht, Germany). Draining lymph node cells (DLNCs) were isolated from rats immunized with guinea pig myelin basic protein (50 μg/rat; kind gift from Professor Alexander Flügel, University of Göttingen, Göttingen, Germany), emulsified with equal volume of CFA. The animals were injected intradermally into hind footpads with 100 μl MBP + CFA. The isolation took place 7 d postimmunization. In some experiments, rats were treated with EP (Sigma-Aldrich) or vehicle (PBS), once per day (i.p., 150 mg/kg body weight), starting from the day of immunization. DLNCs were cultured in RPMI 1640 culture medium (PAA Laboratories, Pasching, Austria) that was supplemented with 2% rat serum. The cells were seeded at 5×10^6/ml in 24-well plates. Spinal cord immune cells (SCICs) were isolated from rats immunized with SCH + CFA, as described previously (29). In brief, rats were extensively perfused with cold PBS before spinal cord isolation. Spinal cords were homogenized and homogenates were centrifuged using 30/70% gradient of Percoll (Sigma-Aldrich). After centrifugation, SCICs were recovered from the Percoll interface and washed in RPMI 1640 medium (PAA Laboratories). SCICs were seeded at 2.5×10^6/ml in 24-well plates. In some experiments, rats were treated with EP or vehicle, once per day (i.p., 300 mg/kg body weight), starting from the day of immunization, and SCICs were isolated at the peak of the disease. Resident peritoneal cells were collected by peritoneal lavage with 3 ml cold PBS from female rats (2–3 mo of age). The cells were counted and seeded in RPMI 1640 culture medium supplemented with 5% heat-inactivated FCS (PAA Laboratories) into 24-well plates (2×10^6/well). After 2 h of incubation at 37˚C in a humidified atmosphere containing 5% CO_2, peritoneal cells were washed two times with PBS to remove nonadherent cells. The adherent cells were considered as purified peritoneal macrophages (PMs). Bone marrow–derived macrophages (BMDMs) were isolated from female rats (2–3 mo of age) as described previously (30). In brief, bone marrow cells were flushed from femurs, seeded at 1×10^6/ml in 24-well plates, and grown for 7 d in the presence of L929 cell supernatant. Adherent cells were used at the end of this period. PM and BMDM purity were assessed by flow cytofluorometry analysis on a CyFlow Space flow cytometer (Partec, Munster, Germany). There was <5% of $CD3^+$ and $CD45R^+$ cells in the purified populations. Microglial BV2 cells were propagated and trypsinized for seeding in 24-well plates (1 or 3×10^5/well). Astrocytes were isolated from mixed glial cell cultures prepared from brains of newborn Dark Agouti rats as previously described (31). They were grown in RPMI 1640 culture medium supplemented with glucose (4 g/l) and purified via repeated trypsinization (0.25% trypsin and 0.02% EDTA; both from Sigma-Aldrich) and replating. Cells were obtained after third passage and were >95% positive for glial fibrillary acidic protein and <3% positive for CD11b, as established by cytofluorimetric analysis. Astrocytes were seeded in 24-well plates at 1.5×10^5/ml/well. For the treatment of cell cultures, the following reagents were used: EP, DMF, LPS, PMA, Con A, recombinant mouse IFN-γ (Sigma-Aldrich), recombinant rat IFN-γ, recombinant mouse IL-17 (R&D Systems, Minneapolis, MN), tetanus toxoid (TT), and tuberculin purified protein derivative (PPD; Torlak, Belgrade, Serbia). In all experiments, EP and DMF were applied simultaneously with stimulation.

Cell viability assays

Viability of DLNCs was assessed by mitochondrial activity assay, that is, mitochondria-dependent reduction of MTT (Sigma-Aldrich) to formazan. At the end of the treatment, DLNCs were collected in tubes, spun down, and supernatants were removed. Cell pellets were dissolved in 0.5 μg/ml MTT solution and incubated for 30 min at 37˚C. Cells were centrifuged and DMSO was added to the pellets to dissolve the formazan crystals. Crystal violet test was applied to assess the viability of macrophages, astrocytes, and BV2 cells. At the end of the treatment, cells were washed with PBS to remove nonadherent dead cells, and the remaining cells were fixed with methanol. After staining with 1% crystal violet solution, the plates were thoroughly washed and then the dye was dissolved in 33% acetic acid. In both assays, the absorbance of dissolved dyes, corresponding to the number of viable cells, was measured at 540 nm with a correction at 690 nm, using an automated microplate reader (LKB 5060-006; LKB, Vienna, Austria).

Detection of NO release and ROS generation

Nitrite accumulation, a measure of NO release, was determined in cell culture supernatants using the Griess reaction. In brief, triplicate aliquots of cell-free supernatants were mixed with an equal volume of Griess reagent (1:1 mixture of 0.1% naphthylethylenediamine dihydrochloride and 1% sulphanilamide in 5% H_3PO_4). The absorbance at 540 nm was determined with a microplate reader and compared with a standard curve for $NaNO_2$. For detection of ROS generation, dihydrorhodamine 123 (Sigma-Aldrich) staining was performed. The cells were pretreated with EP or DMF for 24 h, then incubated in the presence of 1 μM dihydrorhodamine 123 for 30 min and stimulated with PMA for an additional 90 min. The fluorescence was acquired via flow cytometry.

ELISA test for determination of cytokines

Cytokine concentration in cell culture supernatants was determined by sandwich ELISA using MaxiSorp plates (Nunc, Rochild, Denmark) and anti-cytokine paired Abs according to the manufacturer's instructions. Samples were analyzed in duplicates for murine TNF, murine IL-6, rat IL-6, rat IFN-γ (R&D Systems), rat TNF (BD Biosciences, San Diego, CA), and murine/rat IL-17 (eBioscience, San Diego, CA). Lower limit of detection was 30 pg/ml, whereas upper limit of detection was 10 ng/ml for all of the ELISA tests performed. Samples that showed values over the upper limit of detection were adequately diluted for the measurement. The results were calculated using standard curves made on the basis of known concentrations of the appropriate recombinant cytokines.

Immunoblot

Whole-cell lysates were prepared in a solution containing 62.5 mM Tris-HCl, 2% w/v SDS, 10% glycerol, 50 mM DTT, 0.01% w/v bromophe-

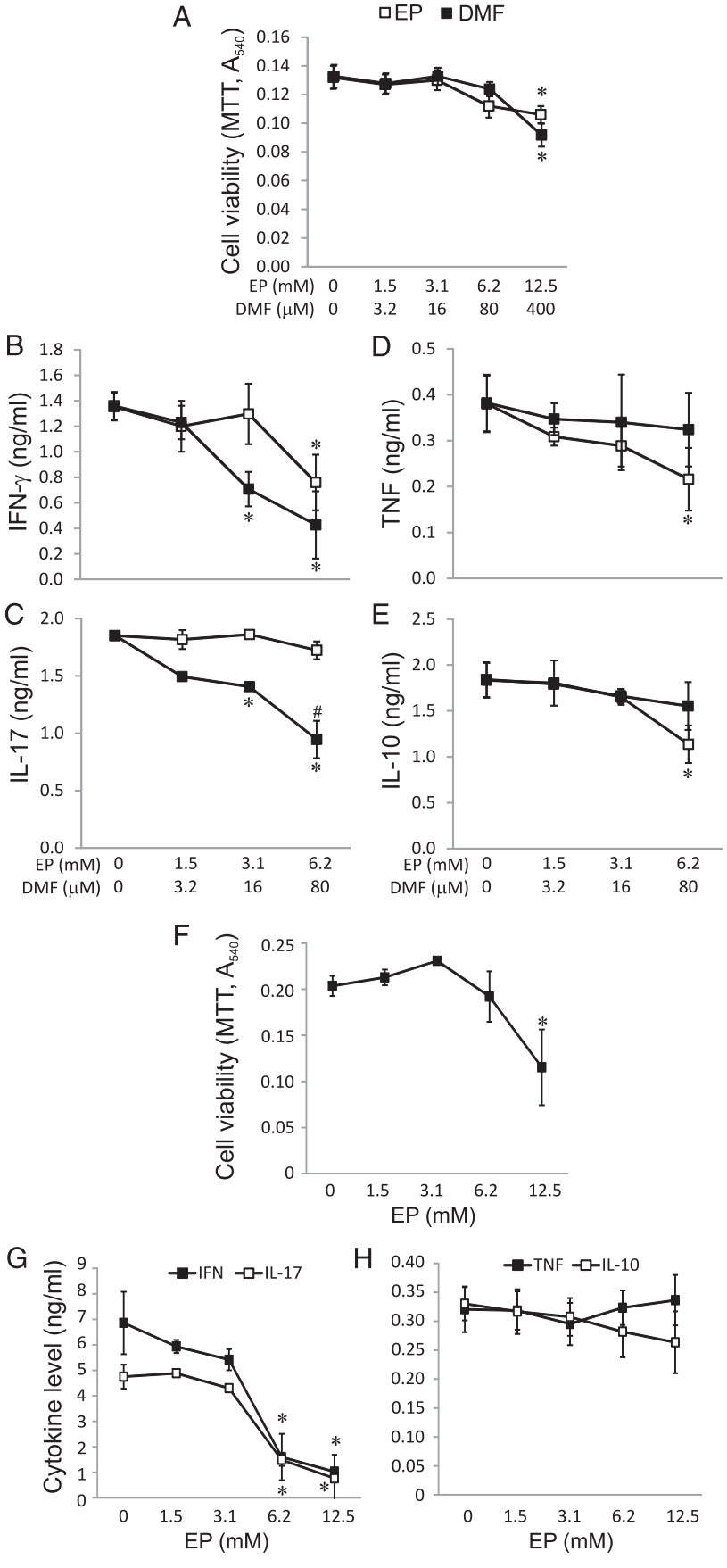

FIGURE 1. Effects of EP and DMF on viability and cytokine release of DLNCs and SCICs. DLNCs (**A**–**E**) were isolated from immunized rats on day 7 post immunization and stimulated with MBP (10 μg/ml) for 48 h. SCICs (**F**–**H**) were isolated from immunized rats at the peak of EAE, and they were cultivated for 48 h. Data are presented as mean ± SD from three independent experiments. $^{*}p < 0.05$, statistically significant compared with medium (0) cultures. $^{\#}p < 0.05$, significant difference between cultures treated with the highest nontoxic doses of DMF and EP.

nol blue, 1 mM phenylmethanesulfonyl fluoride or PMSF, 1 μg/ml aprotinin, and 2 mM EDTA (pH 6.8). Samples containing 20 μg proteins (measured by Lowry protein assay) were electrophoresed on a 12% SDS-polyacrylamide gel. The samples were electrotransferred to polyvinylidene difluoride membranes at 5 mA/cm^2, using semidry blotting system (Fast-blot B43; Biorad, Muenchen, Germany). The blots were blocked with 5% w/v nonfat dry milk in PBS with 0.1% Tween 20 and probed with specific Abs for phosphorylated IkB and β-actin (Cell Signaling Technology, Boston, MA), followed by incubation with the secondary Ab (ECL donkey anti-rabbit HRP-linked; GE Healthcare, Buckinghamshire, U.K.). Detection was performed by the chemiluminescence (ECL; GE Healthcare), and photographs were made by X-ray films (Kodak, Rochester, NY). Densitometry was performed with Scion Image Alpha 4.0.3.2 (Scion Corporation, Frederick, MD).

Cytofluorometry for detection of cell-surface and intracellular markers, apoptosis, and phagocytosis

Cells were stained with PE-conjugated anti-CD4, FITC-conjugated anti-CD11b, anti-CD40, and anti-CD134 (OX40) (BD Biosciences), FITC-conjugated anti-CD8, anti-CD62L, anti-CD25, anti-CD80 and PE-conjugated anti-CD86 (AbD Serotec, Oxford, U.K.), and PE-conjugated anti-F4/80 and anti–MHC class II Abs (eBioscience). Foxp3 staining was performed according to procedure suggested by the manufacturer (eBioscience). Appropriate isotype control Abs were used where necessary to set gates for cell marker positivity. Typically, proportion of isotype control Ab-stained cells was <1%. Detection of apoptosis of DLNCs was performed via Annexin V-FITC staining (Biotium, Hayward, CA). Cells positive for Annexin V-FITC were considered apoptotic. For detection of phagocytosis, BV2 cells were plated in 24-well plates at 1×10^5/well and incubated at 37°C for 1 h. Latex beads (1 μm, yellow-green; Sigma-Aldrich) were preopsonized in PBS supplemented with 50% FCS. The preopsonized beads were added to BV2 cells (10 beads/cell), and cells were incubated at 37°C for an additional hour in the presence of appropriate treatments. BV2 cells were trypsinized for cytofluorometry (Partec CyFlow Space cytometer). Results of cytofluorometry are presented as proportion of cells bound by an appropriate Ab or as mean fluorescent intensity of cell population.

EPR spectroscopy

Electron paramagnetic resonance (EPR) assay for free thiols was applied to establish the affinity of DMF and EP for thiol groups. In brief, reduced glutathione (GSH; 50 μM; Merck, Darmstadt, Germany) was incubated for 2 min with different concentrations of EP or DMF (0–5 mM range) in PBS (pH 7.4). Then thiol-sensitive biradical spin probe RSSR (Enzo Life Sci-

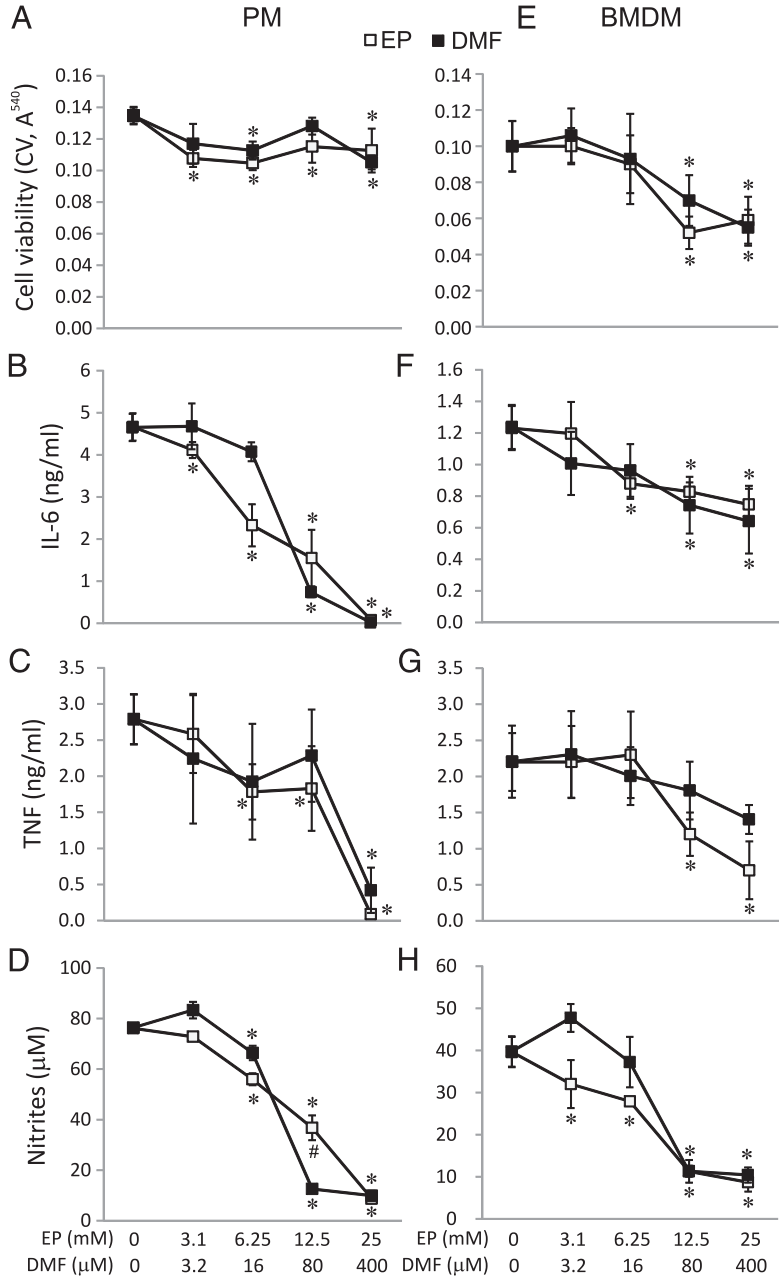

FIGURE 2. Effects of EP and DMF on viability and cytokine and NO production in stimulated macrophages. PMs (**A**–**D**) and BMDMs (**E**–**H**) were stimulated with LPS (100 ng/ml) for 24 h. Mean values ± SD from three independent experiments are presented. *$p < 0.05$, statistically significant compared with medium (0) cultures. $^{\#}p < 0.05$, significant difference between cultures treated with the highest nontoxic dose of DMF and EP.

ences International, Plymouth Meeting, PA) dissolved in DMSO was added to a final concentration of 100 mM. This probe forms an adduct with thiol groups and gives a characteristic EPR spectrum that is used for the quantification of free thiol groups (32). Samples were placed in Teflon tubes with a wall thickness of 0.025 mm and an internal diameter of 0.6 mm (Zeus Industries, Raritan, NJ) and inserted into quartz capillaries. EPR spectra were recorded after 4-min incubation (total) using a Varian E104-A EPR spectrometer operating at X-band (9.51 GHz), EW software (Scientific Software, Bloomington, IL), and the following settings: modulation amplitude, 1 G; modulation frequency, 100 kHz; microwave power, 10 mW; scanning time, 2 min. The concentration of free thiol groups was determined via calibration curve that was prepared using different concentrations of GSH (without DMF or EP).

The ability of EP and DMF to scavenge superoxide radical anion was examined using SOTS-1 (Cayman Chemicals, Ann Arbor, MI), a thermal source of superoxide. SOTS-1 was dissolved in DMSO and supplemented (0.2 mM final concentration) to PBS containing spin trap 5-diethoxyphosphoryl-5-methyl-1-pyrroline-*N*-oxide (DEPMPO; 10 mM; Enzo Life Sciences International) and diethylene triamine pentaacetic acid (1 mM; chelating agent, added to suppress redox activity of transition metals impurities). This system was incubated at 37°C for 5 min in the absence (control system) or the presence of EP (1 or 10 mM) or DMF (1 mM). EPR spectra were acquired 2 min after. The ability of EP and DMF to scavenge hydroxyl radicals ($^{\bullet}OH$) was tested using the Fenton reaction as an $^{\bullet}OH$-producing system ($Fe^{2+} + H_2O_2 \rightarrow Fe^{3+} + OH^- + {}^{\bullet}OH$). The Fenton reaction was performed by combining H_2O_2 (1 mM; Carlo Erba Reagents, Milan, Italy) and $FeSO_4$ (0.2 mM; Merck) in the absence or the presence of EP (1 or 10 mM) or DMF (1 mM). DEPMPO was added before H_2O_2 at the final concentration of 10 mM. The period between the initiation of reaction and EPR measurements was 2 min. In EPR spin-trapping experiments, spectra were recorded using the following settings: modulation amplitude, 2 G; modulation frequency, 100 kHz; microwave power, 10 mW; scanning time, 4 min. Signal intensities were established by simulation and double integration that were performed using WINEPR SimFonia Computer Program (Bruker Analytische Messtechnik GmbH, Karlsruhe, Germany) and previously described simulation parameters (33). Relative inhibition of free radical production was calculated as follows: $(I_{Control} - I_{DMF\ or\ EP})/I_{Control} \times 100$, where I is the intensity of EPR spectrum obtained in controls, or samples with EP or DMF.

Statistical analysis

The results are presented as mean ± SD of values obtained in repeated experiments. A Student *t* test (two-tailed) was performed for statistical analysis. A p value <0.05 was considered statistically significant.

Results

Effects on DLNCs and SCICs

Fig. 1 shows comparison of in vitro effects of EP and DMF on DLNCs that were isolated from rats 7 d after immunization with MBP + CFA and restimulated with MBP in vitro. Significant inhibition of DLNC viability emerged at concentrations of 12.5 mM and 400 μM for EP and DMF, respectively (Fig. 1A). The levels of various cytokines were determined in supernatants of DLNCs treated with EP and DMF at concentrations that did not significantly affect viability. EP reduced the release of IFN-γ (Fig. 1B) and TNF (Fig. 1D). It had no effect on IL-17 production (Fig. 1C), and affected IL-10 release only at the highest concentration tested (Fig. 1E). DMF decreased IFN-γ and IL-17 release (Fig. 1B, 1C) and did not show significant effects on TNF and IL-10 (Fig. 1D, 1E). Fig. 1 also shows in vitro effects of EP on SCICs isolated from rats at the peak of EAE (12–14 d post immunization). Although EP exerted limited effect on SCIC viability (Fig. 1F), it potently inhibited IFN-γ and IL-17, but not IL-10 and TNF, production in these cells (Fig. 1G, 1H). Thus, EP is efficient in the reduction of release of important effector cytokines from in vitro and in vivo reactivated T cells.

Effects on macrophages

Fig. 2 shows the effects of EP and DMF on PMs and BMDMs that were isolated from healthy rats and stimulated with LPS. Both compounds had significant, yet limited inhibitory effects on PM viability at almost all applied concentrations (Fig. 2A). Toxic effects of EP and DMF on BMDMs were more noticeable and emerged at 12.5 mM and 80 μM, respectively (Fig. 2E). Both compounds had profound inhibitory effects on the release of proinflammatory cytokines IL-6 and TNF in PMs (Fig. 2B, 2C) and BMDMs (Fig. 2F, 2G). Also, EP and DMF inhibited NO release in both types of macrophages (Fig. 2D, 2H). Further analyses were performed using EP and DMF concentrations that did not affect the viability of PMs and BMDMs. It can be observed that EP, as well as DMF, suppressed ROS production in PMs (Fig. 3A) and BMDMs (Fig. 3D). Also, we examined the effects of EP and DMF on MHC class II, CD80, CD86, and CD11b expression in PMs and BMDMs. EP and DMF significantly reduced proportion of macrophages expressing MHC class II molecules and downregulated CD11b expression in PMs (Fig. 3B, 3C) and BMDMs (Fig. 3E, 3F). The proportion of cells expressing CD80 and CD86 was not affected (data not shown).

Effects on microglia

EP was not toxic to microglial cells even at a concentration of 25 mM, whereas DMF affected the viability at concentrations as low as 80 μM (Fig. 4A). In the noncytotoxic concentration range, EP showed considerably pronounced effects on the release of IL-6 and TNF from IFN-γ + LPS–stimulated BV2 cells, compared with DMF (Fig. 4B, 4C). EP was superior to DMF in inhibiting NO release as well (Fig. 4D). Further analyses were performed on BV2 cells treated with EP and DMF at nontoxic concentrations. Neither EP nor DMF inhibited ROS generation (Fig. 5A). Phagocytosis was significantly reduced in BV2 cells by EP, but not

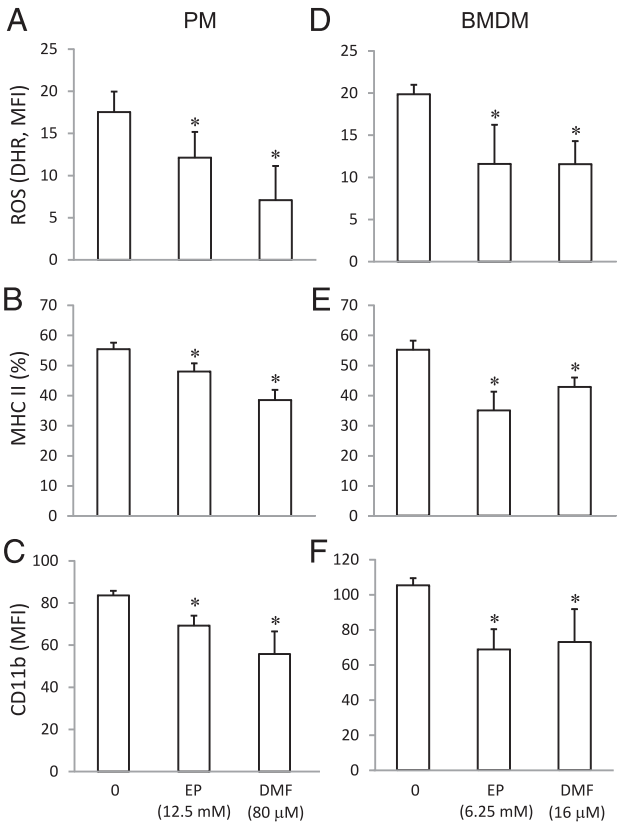

FIGURE 3. Effects of EP and DMF on ROS generation and MHC class II and CD11b expression in stimulated macrophages. PMs (**A**–**C**) and BMDMs (**D**–**F**) were stimulated with LPS (100 ng/ml) for 24 h. For ROS detection, cells were additionally stimulated with PMA (400 ng/ml). Mean values ± SD from three independent experiments are presented. *$p <$ 0.05, statistically significant compared with medium (0) cultures.

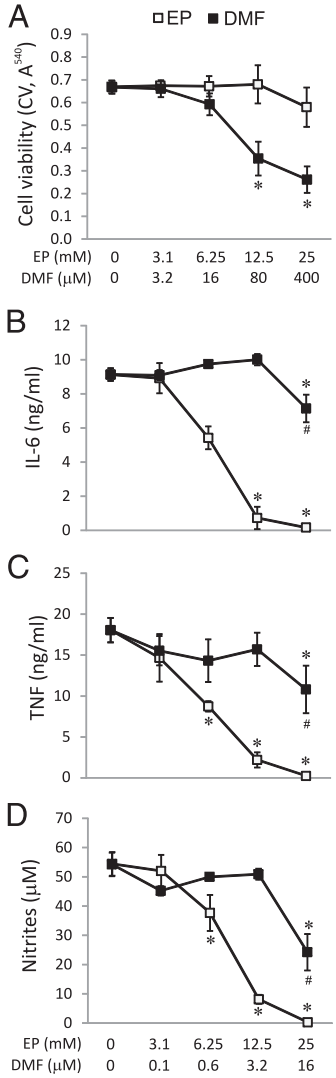

FIGURE 4. Effects of EP and DMF on viability (**A**), cytokine (**B** and **C**), and NO (**D**) production in stimulated BV2 cells. BV2 cultures were stimulated with LPS (100 ng/ml) and IFN-γ (10 ng/ml) for 24 h. Mean values ± SD from three independent experiments are presented. $^{*}p < 0.05$, statistically significant compared with medium (0) cultures. $^{\#}p < 0.05$, significant difference between cultures treated with the highest nontoxic dose of DMF and EP.

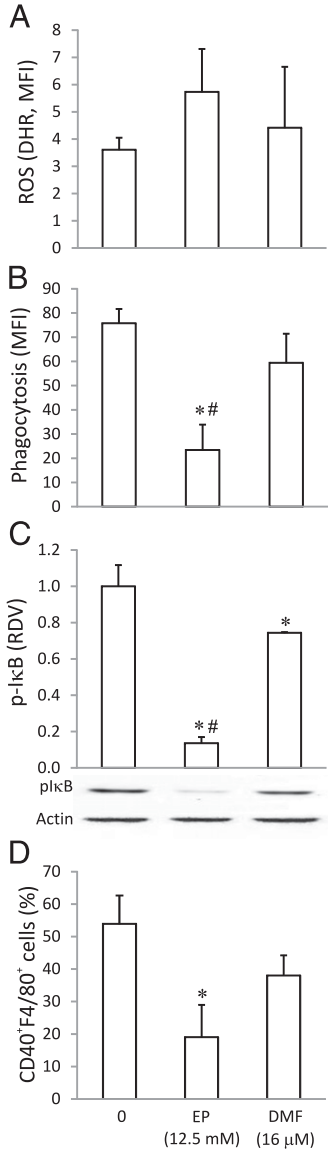

FIGURE 5. Effects of EP and DMF on stimulated BV2 cells. ROS production (cells were additionally stimulated with 400 ng/ml PMA) (**A**), phagocytosis (**B**), the level of phosphorylated IκB (**C**), and expression of CD40 and F4/80 (**D**) were determined in cells stimulated with LPS (100 ng/ml) and IFN-γ (10 ng/ml) in the absence or the presence of EP (12.5 mM) or DMF (16 μM) for 24 h. Mean values ± SD from three independent experiments are presented. $^{*}p < 0.05$, statistically significant compared with medium (0) cultures. $^{\#}p < 0.05$, significant difference between cultures treated with DMF and EP.

by DMF (Fig. 5B). The effects of EP and DMF on NF-κB activation in IFN-γ + LPS–stimulated microglial cells were determined via detection of phosphorylated, that is, inactivated NF-κB inhibitory molecule, IκB. It can be observed that both EP and DMF inhibited NF-κB activation via increasing the level of active IκB, yet the effects of EP were significantly more pronounced compared with DMF (Fig. 5C). Finally, EP, and to a lesser extent DMF, reduced the proportion of BV2 cells expressing activation markers CD40 and F4/80 (Fig. 5D).

Effects on astrocytes

It appears that both compounds were more toxic to astrocytes compared with other cell types investigated in this study. However, whereas toxic doses of EP were in the millimolar range (>6.25 mM), those of DMF were in micromolar range (≤16 μM; Fig. 6A). Level of a proinflammatory cytokine IL-6 was reduced in the cell cultures treated with concentrations of EP or DMF that did not affect astrocyte viability (Fig. 6B). Last, only EP provoked significant inhibition of NF-κB activation by suppressing IκB phosphorylation (Fig. 6C). In summary, EP is less toxic than DMF to astrocytes in vitro, and it blocks IL-6 generation and NF-κB activation in these cells.

Thiol-binding and antioxidative capacities

An EPR spin-probing assay was applied to examine capacities of EP and DMF to form thiol adducts. The steeper concentration-adduct formation curve for DMF compared with EP implies that DMF has a higher affinity for thiols (Fig. 7A). Besides thiol-adducts–mediated activation/inhibition of complex cellular responses, EP and DMF might act as blunt antioxidants. In line with this, we examined their capacities to scavenge two pathologically most relevant-free radicals: superoxide and hydroxyl radical. For this purpose, specific generating systems and spin-trapping method were applied. In this technique, an EPR "silent"

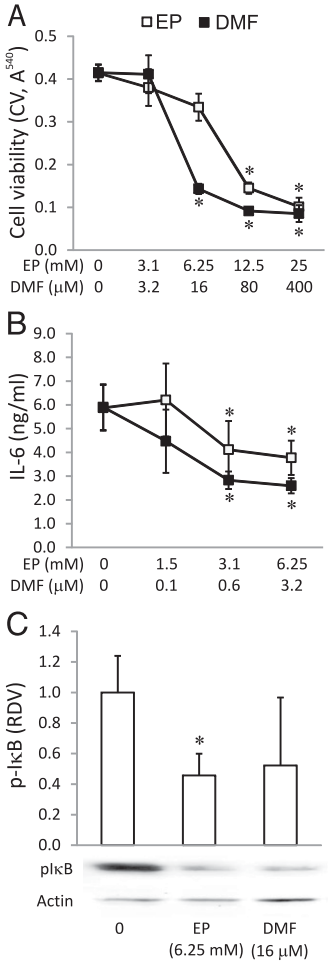

FIGURE 6. Effects of EP and DMF on stimulated astrocytes. Viability (**A**), IL-6 concentration (**B**), and level of pIkB (**C**) were determined in astrocytes that were stimulated with IFN-γ (10 ng/ml) and IL-17 (50 ng/ml) for 24 h in the presence or the absence of EP or DMF. Mean values ± SD from three independent experiments are presented. $*p < 0.05$, statistically significant compared with medium (0) cultures.

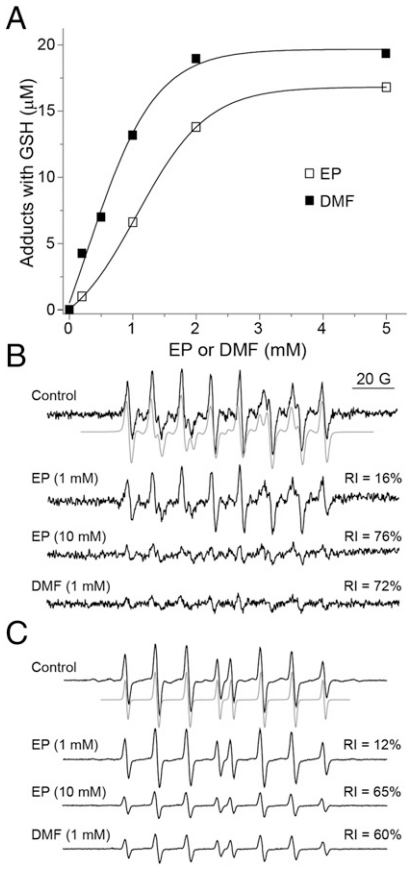

FIGURE 7. Redox properties of EP and DMF. The ability to bind to thiol groups on GSH. Curves represent sigmoidal fits (**A**). Characteristic EPR signals of DEPMPO adduct with superoxide in the absence or the presence of EP or DMF (**B**). Characteristic EPR signals of DEPMPO adduct with hydroxyl radical in the absence or the presence of EP or DMF (**C**). Gray represents spectral simulations, which were applied to evaluate signal intensities (I). Relative inhibition (RI) was calculated according to the formula: $(I_{Control} - I_{DMF\ or\ EP})/I_{Control} \times 100$ from three independent experiments.

compound, spin trap (DEPMPO in this study), is added to the sample to react with radicals and form stable EPR active spin adducts exhibiting characteristic EPR spectra. A decrease in the intensity or EPR signal stands for a lower level of free radicals in the system. Fig. 7B shows that DMF at 1 mM (well above the cytotoxic level) drastically decreased EPR signal of DEPMPO adduct with superoxide. EP showed modest effects at the same concentration but reached antioxidative performance of DMF at 10-fold higher concentration. A very similar setup was observed for hydroxyl radical, that is, the ability of DMF to remove this ROS was ~10-fold more pronounced compared with EP (Fig. 7C).

Effects on EAE in rats

Rats were immunized with SCH + CFA and treated once per day with EP (300 mg/kg) or vehicle (eight animals per group) starting 1 d before the expected clinical onset of the disease until the end of the first relapse (day 17). Whereas control (vehicle-treated) rats developed full-blown EAE with a strong first attack and consequent relapse of the disease, EP-treated rats had a mild first attack and no relapse until the end of the observation period (day 40 post immunization; Fig. 8A). EAE started earlier and lasted longer in the control group, whereas cumulative c.s., maximal c.s., and average c.s. were significantly lower in the EP-treated group (Table I). A drastically lower number of SCICs was obtained from whole spinal cord isolates of EP-treated rats ($0.71 \pm 0.25 \times 10^6$) compared with vehicle-treated rats ($2.03 \pm 0.29 \times 10^6$). Furthermore, SCICs from EP-treated animals produced less IL-17 than corresponding cells isolated from the control rats (Fig. 8B). Finally, the effects of in vivo application of EP in the inductive phase of EAE on cytokine generation in DLNCs were examined. There was a slight but nonsignificant decrease in the number of DLNCs that were isolated from EP-treated ($31.9 \pm 13.7 \times 10^6$/DLN) compared with control rats ($36.6 \pm 13.4 \times 10^6$/DLN). Further, there was no difference in the viability of DLNCs isolated from EP-treated and vehicle-treated rats after 48 h of cultivation in the absence or presence of MBP as determined by MTT test (data not shown). However, DLNCs isolated from EP-treated rats produced significantly less IFN-γ and IL-17 in MBP-stimulated and in nonstimulated cultures (Fig. 8C). TNF and IL-10 release ex vivo was not affected by EP in neither SCICs nor DLNCs. Frequencies of various cellular populations among DLNCs were determined by flow cytofluorometry (Table II). EP induced a significant increase in the number of $CD4^+CD25^+$ cells. Still, this was not accompanied by the rise in the frequency of DLNCs expressing Foxp3, the signature marker of regulatory T cells. The proportions of other relevant phenotypes were not significantly modulated by in vivo treatment with EP, including the frequency of naive CD4 T cells ($CD4^+CD62L^+$) and activated CD4 T cells ($CD4^+OX40^+$). Of note, there was no influence of EP on the frequency of apoptotic

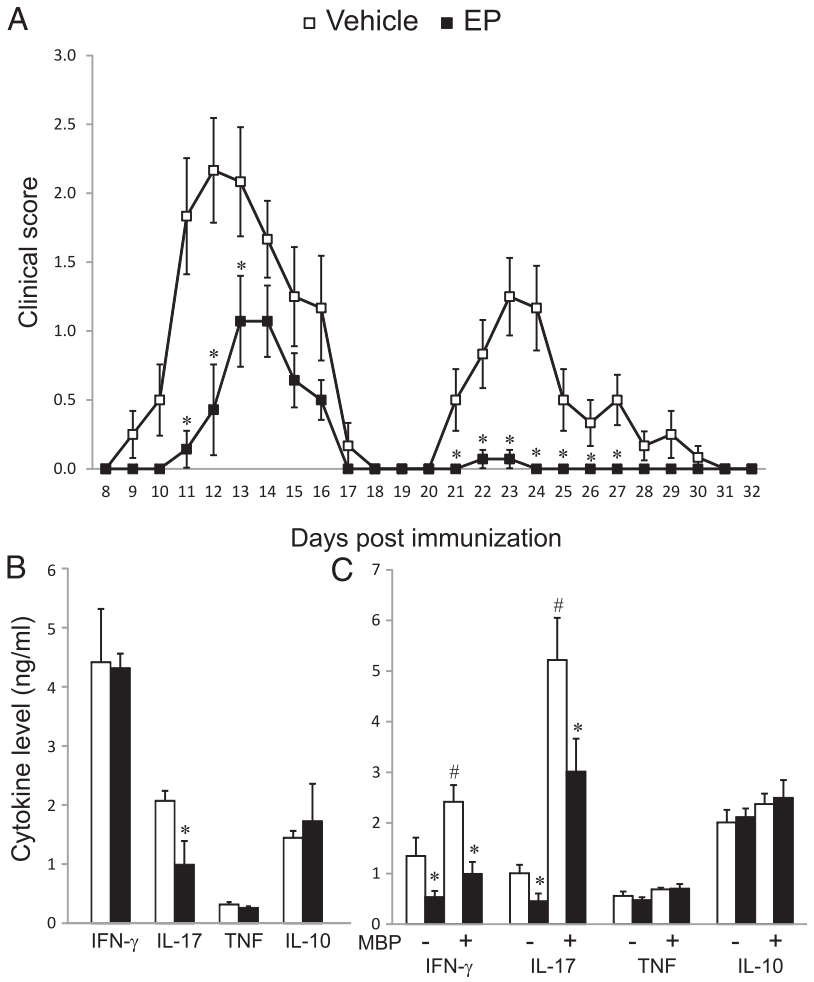

FIGURE 8. Effects of EP on EAE. Immunized rats were treated once per day with EP or vehicle from day 8 until day 17 post immunization (**A**), from day 8 to the peak of the disease (**B**), or from days 0 to 7 post immunization (**C**). SCICs were isolated at the peak of the disease, and viability and cytokine production were determined after 48 h of cultivation (B). DLNCs were isolated on day 7 post immunization and cultivated in medium alone (0) or restimulated in vitro with MBP (10 μg/ml) for 48 h (C). Mean values ± SD from eight rats (A) or from six rats (B and C) per group are presented. $^{*}p < 0.05$, statistically significant compared with samples of vehicle-treated rats. $^{\#}p < 0.05$, significant difference between corresponding untreated (0) and MBP-restimulated cultures.

cells among DLNCs or $CD4^+$ T cells purified from DLNCs (Table II). In close, EP potently modulated encephalitogenic cells within the CNS and at the periphery, and consequently alleviated relapsing-remitting EAE in rats.

Effects on human PBMCs

Human PBMCs were stimulated with a mitogen (Con A) or with Ags (TT or PPD) in the presence or absence of EP. Viability of human PBMCs stimulated with Con A was affected only at 25 mM EP (Fig. 9A). At the same time, the production of IFN-γ and IL-17 was potently inhibited by EP in concentrations that did not reduce PBMC viability (Fig. 9B, 9C). Moreover, at the dose that was not toxic to PBMCs (Fig. 9D), EP significantly reduced IFN-γ and IL-17 production in Ag-stimulated PBMCs (Fig. 9E, 9F).

Discussion

We showed in this study that EP and DMF have in common a number of MS-relevant anti-inflammatory effects. Of major interest in this study is the suppressed release of T cell effector cytokines: IFN-γ and IL-17. These cytokines represent the markers of Th1 and Th17 cells, which have been considered the major driving force of inflammation and autoimmunity in MS (24). EP and DMF provoked a drop in macrophage release/production of cytokines (IL-6 and TNF) and reactive species (NO and ROS), which promote neuroinflammatory and neurodegenerative events in MS. For example, it has been shown that IL-6 potentiates the resistance of effector T cells to regulatory T cells in MS (34), and that soluble TNF actively contributes to demyelination and axonal degeneration in EAE neuroinflammation (35). Likewise, NO and different ROS are involved in oligodendrocytes loss, blood–brain barrier dysfunction, T cell infiltration, and neurodegeneration (5). The essential role of macrophages in MS pathology via Ag presentation and epitope spreading has been outlined recently (36). Pertinent to this, EP and DMF obstructed MHC class II expression in macrophages. Also, the ability of EP and DMF to scavenge ROS and to inhibit NO and ROS generation

Table I. Effects of EP on EAE parameters

Treatment	Incidence (%)	Onset (d)	Duration (d)	Cumulative c.s.	Average c.s.	Maximal c.s.
1st Episode						
Vehicle	100.0	10.2 ± 1.0	4.8 ± 1.0	11.1 ± 3.3	2.3 ± 0.7	2.8 ± 0.7
EP	87.5	12.7 ± 1.0*	2.0 ± 1.3*	3.9 ± 3.2*	1.5 ± 0.9	1.1 ± 0.9*
Relapse						
Vehicle	100.0	21.7 ± 0.8	5.7 ± 3.4	5.6 ± 4.2	0.9 ± 0.3	1.3 ± 0.7
EP	12.5	22.3 ± 0.5	0.4 ± 0.8*	0.1 ± 0.4*	0.1 ± 0.2*	0.1 ± 0.2*

Mean values ± SD from eight rats per group are presented.
$^{*}p < 0.05$, statistically significant compared with samples of vehicle-treated EAE rats.

Table II. Phenotypic analysis of DLNCs isolated from immunized rats treated with EP

	Control	EP
$CD4^+$	44.3 ± 3.4	40.8 ± 4.2
$CD8^+$	15.8 ± 4.9	16.9 ± 1.4
$CD4^+CD8^+$	1.9 ± 0.4	1.9 ± 0.5
$CD4^+CD62L^+$	36.4 ± 2.1	36.9 ± 2.7
$CD4^+OX40^+$	7.0 ± 0.8	8.5 ± 0.7
$CD4^+CD25^+$	4.5 ± 0.4	5.2 ± 0.3*
$CD4^+CD25^+$ $Foxp3^+$	2.7 ± 0.2	3.0 ± 0.3
$MHCII^+$	5.3 ± 1.7	5.2 ± 0.9
$CD80^+$	ND	ND
$MHCII^+CD80^+$	9.7 ± 0.6	8.9 ± 1.4
$CD11b^+$	7.5 ± 0.2	8.3 ± 0.8
$CD86^+$	0.8 ± 0.1	0.9 ± 0.1
$CD11b^+CD86^+$	1.5 ± 0.1	1.8 ± 0.2
DLNCs (apoptotic)	12.8 ± 2.8	11.8 ± 3.9
$CD4^+$ T cells (apoptotic)	16.4 ± 2.6	14.8 ± 4.2

Ab staining was performed immediately after isolation. Data (%) are presented as mean ± SD from four DLN per group.
*$p < 0.05$, statistically significant difference between EP and Ctrl.
ND, not detected.

might add to their anti-Ag–presenting effects, as it is known that macrophages use ROS and NO in myelin processing, whereas reactive species appear to contribute to the generation of new epitopes in MS (5). In addition, EP and DMF downregulated the expression of CD11b, an adhesion molecule that is critical for the development of EAE (37).

In IFN-γ + LPS–stimulated microglial cells, EP and DMF suppressed IL-6, TNF, and NO release, and NF-κB activation. Importantly, the effects of EP, but not DMF emerged at concentrations that did not affect cell viability. Thus, the observed effects of EP were not a consequence of fewer producers, but rather of lowered capacity to produce the cytokines and NO. The effects of EP on NF-κB and NO generation are most likely interlinked. It is known that NF-κB controls the expression of inducible NO synthase (iNOS) (38), and that iNOS expression can be reduced in activated microglia via suppression of IκB phosphorylation, which leads to NF-κB inhibition (39). Of note, our findings are in accordance with available data on the effects of DMF on IL-6, TNF, and NO production, and the effects of EP on cytokine and NO production, and iNOS expression in LPS-stimulated microglia (13, 19, 40). It appears that pretreatment with EP exerts even more potent effects on LPS-activated primary microglia (19). Further, EP and DMF restrained microglia activation according to: 1) lower number of cells positive for CD40 (costimulatory protein found on APCs), 2) lower number of $F4/80^+$ cells (a marker of mature macrophages), and 3) suppressed phagocytosis. Microglial cells are semiprofessional APCs, and immunomodulatory effects observed in this article might hinder Ag presentation. In IFN-γ + IL-17–stimulated astrocytes, EP and DMF suppressed IL-6 release

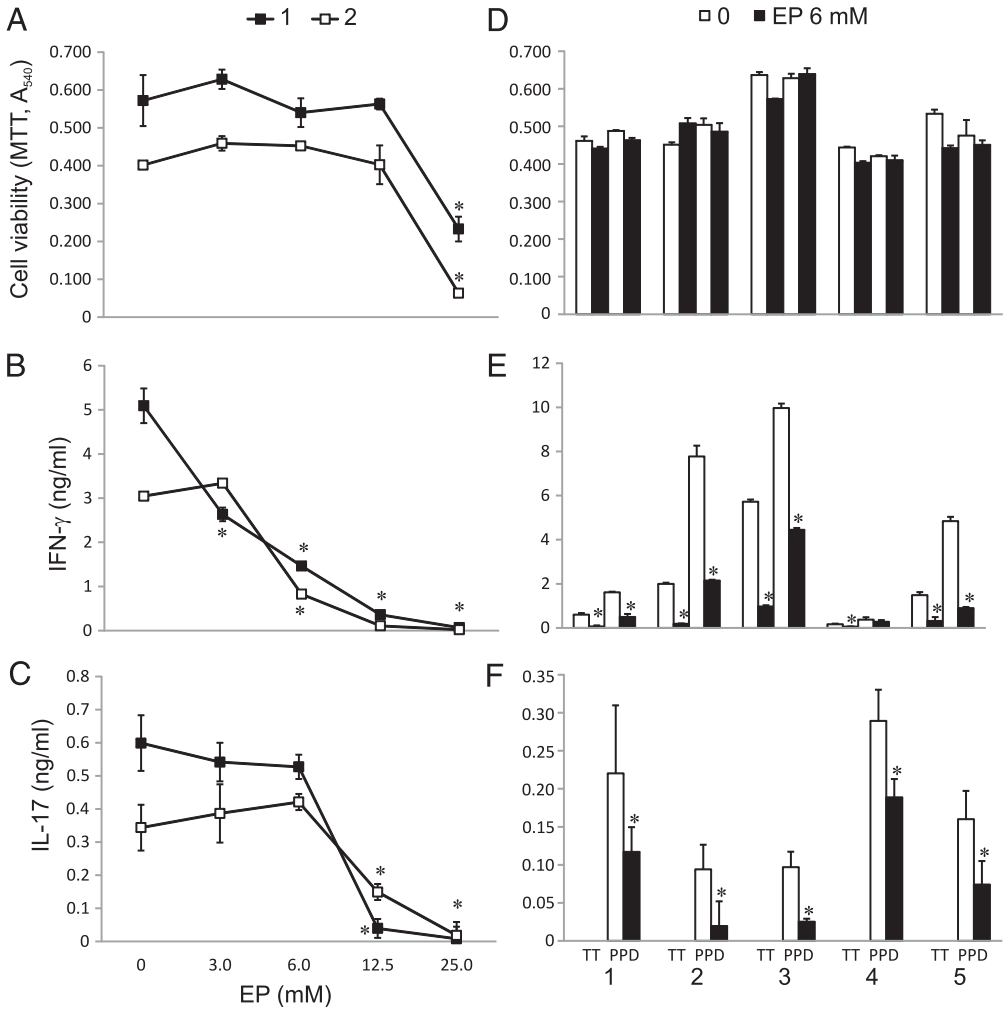

FIGURE 9. Effects of EP on human PBMCs. PBMCs were isolated from healthy volunteers (1–5) and stimulated with Con A (2.5 μg/ml) for 24 h (**A**–**C**) or with TT (2 μg/ml) or PPD (10 μg/ml) for 48 h (**D**–**F**). PBMCs did not produce measurable levels of IL-17 in response to TT. Data are presented as means ± SD from triplicate measurements. *$p < 0.05$, statistically significant compared with medium (0) cultures.

and NF-κB activation. This is similar to previous reports showing decreased IL-6 release (40) and preserved IκB inhibitory performance in LPS-stimulated astrocytes exposed to DMF (4). The study by Lin and coauthors (4) documented that this and other effects of DMF are mediated via thiol-binding. In respect to this, we showed in this study that EP shows the affinity for thiol groups as well. Pertinent to MS, the activation of NF-κB is a well-known feature of astrocytes in active lesions (41). It has been shown on the cuprizone model of demyelination that the cell-specific inhibition of NF-κB in astrocytes is sufficient to protect the mice from myelin loss (42). The suppression of NF-κB activity in astrocytes might be a very important tool in alleviating neurodegeneration. NF-κB appears to activate a set of pro-oxidative events and self-sustaining redox loops (38), and astrocytes have been postulated to be the centers of oxidative stress in MS lesions (43). Finally, EP and DMF are capable of providing a more direct antioxidative protection via scavenging superoxide and hydroxyl radical, which have the central place in MS-related neurodegenerative processes, such as "slow burning" of demyelinated neurons and oxidative damage directly inflicted by cytotoxic cells (5).

Emerging data imply that EP might be an effective anti-inflammatory agent in vivo. In models of hypoxia-ischemia– and LPS-provoked white matter injury, EP has significantly reduced oligodendrocyte loss and hypomyelination, astrocytes and microglia activation, and proinflammatory cytokine release (44, 45). In an intracerebral hemorrhage-induced brain injury model, EP protected neurons from degeneration, suppressed the activation of microglia, and downregulated the production of TNF and IL-1β (18). EP has shown neuroprotective capacities in a spinal cord injury model. It inhibited astrogliosis and neuroinflammation, promoted neuron survival and neural regeneration, and improved the functional recovery of spinal cord (46). In addition, it has been shown that EP attenuated matrix metalloproteinase 9 expression in the CNS and on the periphery, blood–brain barrier breakdown, cerebral inflammation, and secondary neuronal damage in a traumatic brain injury model (19). Finally, in rats with LPS-induced inflammation (a model of sepsis), EP treatment suppressed IL-6 and TNF levels in plasma (14). In respect to MS, we showed in this study that in vivo treatment of EAE animals with EP potently affects the ability of MBP-specific, that is, encephalitogenic T cells, to produce effector cytokines IFN-γ and IL-17. Moreover, EAE was markedly downregulated in rats treated with EP. It is important to note that EAE animals were treated only during the first relapse, that is, there was no pretreatment with EP, and the application was stopped at the end of the episode. This treatment modality was applied to mimic the therapy of MS patients in relapse. It delivered significantly lower clinical scores, delay of EAE onset, and shorter period of the first attack, but also annihilated the second attack, which implies that EP has long-term anti-inflammatory effects in EAE. Importantly, this treatment lowered the number and activity of immune cells within the CNS, thus probably hampering deleterious effects of neuroinflammation. Interestingly, although application of EP in the inductive phase of EAE led to reduced production of both IFN-γ and IL-17 in DLNCs, the therapeutic treatment restricted only IL-17 generation in SCICs. However, it has to be emphasized that overall production of IFN-γ within the CNS was also reduced because there were less inflammatory cells present in spinal cords of EP-treated rats. In line with this, both IFN-γ and IL-17 production were inhibited in SCICs in vitro. Potency of EP to inhibit synthesis of Th1 and Th17 effector cytokines was further demonstrated in human immune cells, where it was clearly shown that this agent restricted IFN-γ and IL-17 generation in polyclonal and Ag-specific response of human PBMCs. Both in vivo effect of EP in model animals and its in vitro effect on human cells are of relevance for taking EP into consideration as a potential MS therapeutic.

In vitro anti-(neuro)inflammatory effects of EP emerged in the higher concentration range compared with DMF. This also appears to be true for in vivo settings. EP alleviated EAE in model animals at daily doses of 300 mg/kg, whereas recommended oral maintenance dosage of Tecfidera for MS patients is 240 mg twice a day (~6 mg/kg/day). The discrepancy between the effective concentrations/doses of EP and DMF might be explained by the facts that: 1) EP represents a metabolic substrate, that is, intracellular esterase processes EP to pyruvate that is further available for tricarboxylic acid cycle (47); and 2) on the biochemical level, EP showed lower capacity to form thiol-adducts and to scavenge ROS compared with DMF. Nevertheless, the immunomodulatory dose range of EP is still well below the cell toxicity threshold as measured by cell viability. More importantly, EP is approved for human use and has been enrolled in several clinical trials (11, 14). As an illustration, in a U.S.-based clinical trial (the only finished phase II trial on EP so far), six doses of 7.5 g EP were administered i.v. during 36 h (360 mg/kg/day) to high-risk patients undergoing cardiac surgery (48). Although this trial has not delivered clear clinical benefits in the prevention of sepsis and related conditions, it did show that EP is safe and well tolerated at high doses.

Although there are several drugs for MS treatment on the market, none of them is the cure for the disease, and there are significant concerns about their side effects and long-term efficacy (1). Also, these are lifelong therapies with high prices (http://www.healthline.com/health-news/ms-why-are-ms-drug-prices-so-high-071913). All of these facts call upon studies on new drugs that would overcome the common disadvantages of the existing medications. In line with this, the aim of the recently launched MS-Secondary Progressive Multi-Arm Randomization Trial (MS-SMART) is the testing of three off-the-shelf drugs as possible therapeutics for MS (http://www.ms-smart.org). The perspective for development of redox strategy-based MS therapy is open. DMF could be the first-in-class drug, and it appears that EP might be the next in line. Our results speak in favor of this possibility. Maybe the most favorable facts are that EP reduced IFN-γ and IL-17 generation in human PBMCs, alleviated EAE in rats, and even more it practically prevented the second relapse. Still, further research on animal models is needed. Taking into account the importance of redox component in the mechanisms of EP activity, in addition to the widely used EAE, examinations should be focused on the model of coronavirus-induced demyelinating encephalomyelitis. According to a recently published study, this model reflects oxidative processes in MS in the most appropriate way (49). In conclusion, further studies on the possibility to use EP as a MS therapeutic are warranted.

Acknowledgments

We are thankful to Dr. Irena Novaković at the Center for Chemistry, Institute of Chemistry, Technology and Metallurgy, University of Belgrade for technical assistance.

Disclosures

The authors have no financial conflicts of interest.

References

1. Ruggieri, S., C. Tortorella, and C. Gasperini. 2014. Pharmacology and clinical efficacy of dimethyl fumarate (BG-12) for treatment of relapsing-remitting multiple sclerosis. *Ther Clin Risk Manag* 10: 229–239.
2. Linker, R. A., D. H. Lee, S. Ryan, A. M. van Dam, R. Conrad, P. Bista, W. Zeng, X. Hronowsky, A. Buko, S. Chollate, et al. 2011. Fumaric acid esters exert neuroprotective effects in neuroinflammation via activation of the Nrf2 antioxidant pathway. *Brain* 134: 678–692.
3. Schmidt, T. J., M. Ak, and U. Mrowietz. 2007. Reactivity of dimethyl fumarate and methylhydrogen fumarate towards glutathione and N-acetyl-L-cysteine—

preparation of S-substituted thiosuccinic acid esters. *Bioorg. Med. Chem.* 15: 333–342.
4. Lin, S. X., L. Lisi, C. Dello Russo, P. E. Polak, A. Sharp, G. Weinberg, S. Kalinin, and D. L. Feinstein. 2011. The anti-inflammatory effects of dimethyl fumarate in astrocytes involve glutathione and haem oxygenase-1. *ASN Neuro* 3: e00055.
5. Miljković, D., and I. Spasojević. 2013. Multiple sclerosis: molecular mechanisms and therapeutic opportunities. *Antioxid. Redox Signal.* 19: 2286–2334.
6. Gelderman, K. A., M. Hultqvist, J. Holmberg, P. Olofsson, and R. Holmdahl. 2006. T cell surface redox levels determine T cell reactivity and arthritis susceptibility. *Proc. Natl. Acad. Sci. USA* 103: 12831–12836.
7. Yan, Z., and R. Banerjee. 2010. Redox remodeling as an immunoregulatory strategy. *Biochemistry* 49: 1059–1066.
8. Yan, Z., S. K. Garg, and R. Banerjee. 2010. Regulatory T cells interfere with glutathione metabolism in dendritic cells and T cells. *J. Biol. Chem.* 285: 41525–41532.
9. Halliwell, B. 2013. The antioxidant paradox: less paradoxical now? *Br. J. Clin. Pharmacol.* 75: 637–644.
10. Han, Y., J. A. Englert, R. Yang, R. L. Delude, and M. P. Fink. 2005. Ethyl pyruvate inhibits nuclear factor-kappaB-dependent signaling by directly targeting p65. *J. Pharmacol. Exp. Ther.* 312: 1097–1105.
11. Kao, K. K., and M. P. Fink. 2010. The biochemical basis for the anti-inflammatory and cytoprotective actions of ethyl pyruvate and related compounds. *Biochem. Pharmacol.* 80: 151–159.
12. Shin, J. H., S. W. Kim, Y. Jin, I. D. Kim, and J. K. Lee. 2012. Ethyl pyruvate-mediated Nrf2 activation and hemeoxygenase 1 induction in astrocytes confer protective effects via autocrine and paracrine mechanisms. *Neurochem. Int.* 61: 89–99.
13. Kim, S. W., H. K. Lee, J. H. Shin, and J. K. Lee. 2013. Up-down regulation of HO-1 and iNOS gene expressions by ethyl pyruvate via recruiting p300 to Nrf2 and depriving It from p65. *Free Radic. Biol. Med.* 65: 468–476.
14. Fink, M. P. 2007. Ethyl pyruvate: a novel anti-inflammatory agent. *J. Intern. Med.* 261: 349–362.
15. Kalariya, N. M., A. B. Reddy, N. H. Ansari, F. J. VanKuijk, and K. V. Ramana. 2011. Preventive effects of ethyl pyruvate on endotoxin-induced uveitis in rats. *Invest. Ophthalmol. Vis. Sci.* 52: 5144–5152.
16. Tang, H., H. Zhao, J. Song, H. Dong, L. Yao, Z. Liang, Y. Lv, F. Zou, and S. Cai. 2014. Ethyl pyruvate decreases airway neutrophil infiltration partly through a high mobility group box 1-dependent mechanism in a chemical-induced murine asthma model. *Int. Immunopharmacol.* 21: 163–170.
17. Kim, J. B., Y. M. Yu, S. W. Kim, and J. K. Lee. 2005. Anti-inflammatory mechanism is involved in ethyl pyruvate-mediated efficacious neuroprotection in the postischemic brain. *Brain Res.* 1060: 188–192.
18. Su, X., H. Wang, L. Zhu, J. Zhao, H. Pan, and X. Ji. 2013. Ethyl pyruvate ameliorates intracerebral hemorrhage-induced brain injury through anti-cell death and anti-inflammatory mechanisms. *Neuroscience* 245: 99–108.
19. Shi, H., H. L. Wang, H. J. Pu, Y. J. Shi, J. Zhang, W. T. Zhang, G. H. Wang, X. M. Hu, R. K. Leak, J. Chen, and Y. Q. Gao. 2014. Ethyl pyruvate protects against blood-brain barrier damage and improves long-term neurological outcomes in a rat model of traumatic brain injury. *CNS Neurosci. Ther.* 10.1111/cns.12366.
20. Choi, J. S., M. S. Lee, and J. W. Jeong. 2010. Ethyl pyruvate has a neuroprotective effect through activation of extracellular signal-regulated kinase in Parkinson's disease model. *Biochem. Biophys. Res. Commun.* 394: 854–858.
21. di Penta, A., B. Moreno, S. Reix, B. Fernandez-Diez, M. Villanueva, O. Errea, N. Escala, K. Vandenbroeck, J. X. Comella, and P. Villoslada. 2013. Oxidative stress and proinflammatory cytokines contribute to demyelination and axonal damage in a cerebellar culture model of neuroinflammation. *PLoS ONE* 8: e54722.
22. Jang, M., M. J. Lee, and I. H. Cho. 2014. Ethyl pyruvate ameliorates 3-nitropropionic acid-induced striatal toxicity through anti-neuronal cell death and anti-inflammatory mechanisms. *Brain Behav. Immun.* 38: 151–165.
23. Wekerle, H. 2008. Lessons from multiple sclerosis: models, concepts, observations. *Ann. Rheum. Dis.* 67(Suppl. 3): iii56–iii60.
24. Petermann, F., and T. Korn. 2011. Cytokines and effector T cell subsets causing autoimmune CNS disease. *FEBS Lett.* 585: 3747–3757.
25. Chastain, E. M., D. S. Duncan, J. M. Rodgers, and S. D. Miller. 2011. The role of antigen presenting cells in multiple sclerosis. *Biochim. Biophys. Acta* 1812: 265–274.
26. Zindler, E., and F. Zipp. 2010. Neuronal injury in chronic CNS inflammation. *Best Pract. Res. Clin. Anaesthesiol.* 24: 551–562.
27. Miljković, D., G. Timotijević, and M. Mostarica Stojković. 2011. Astrocytes in the tempest of multiple sclerosis. *FEBS Lett.* 585: 3781–3788.
28. Goldmann, T., and M. Prinz. 2013. Role of microglia in CNS autoimmunity. *Clin. Dev. Immunol.* 2013: 208093.
29. Miljković, D., Z. Stanojević, M. Momcilović, F. Odoardi, A. Flügel, and M. Mostarica-Stojković. 2011. CXCL12 expression within the CNS contributes to the resistance against experimental autoimmune encephalomyelitis in Albino Oxford rats. *Immunobiology* 216: 979–987.
30. Boltz-Nitulescu, G., C. Wiltschke, C. Holzinger, A. Fellinger, O. Scheiner, A. Gessl, and O. Förster. 1987. Differentiation of rat bone marrow cells into macrophages under the influence of mouse L929 cell supernatant. *J. Leukoc. Biol.* 41: 83–91.
31. McCarthy, K. D., and J. de Vellis. 1980. Preparation of separate astroglial and oligodendroglial cell cultures from rat cerebral tissue. *J. Cell Biol.* 85: 890–902.
32. Spasojević, I. 2011. Free radicals and antioxidants at a glance using EPR spectroscopy. *Crit. Rev. Clin. Lab. Sci.* 48: 114–142.
33. Pristov, J. B., A. Mitrović, and I. Spasojević. 2011. A comparative study of antioxidative activities of cell-wall polysaccharides. *Carbohydr. Res.* 346: 2255–2259.
34. Schneider, A., S. A. Long, K. Cerosaletti, C. T. Ni, P. Samuels, M. Kita, and J. H. Buckner. 2013. In active relapsing-remitting multiple sclerosis, effector T cell resistance to adaptive T(regs) involves IL-6-mediated signaling. *Sci. Transl. Med.* 5: 170ra15.
35. Brambilla, R., J. J. Ashbaugh, R. Magliozzi, A. Dellarole, S. Karmally, D. E. Szymkowski, and J. R. Bethea. 2011. Inhibition of soluble tumour necrosis factor is therapeutic in experimental autoimmune encephalomyelitis and promotes axon preservation and remyelination. *Brain* 134: 2736–2754.
36. Lucchinetti, C. F., B. F. Popescu, R. F. Bunyan, N. M. Moll, S. F. Roemer, H. Lassmann, W. Brück, J. E. Parisi, B. W. Scheithauer, C. Giannini, et al. 2011. Inflammatory cortical demyelination in early multiple sclerosis. *N. Engl. J. Med.* 365: 2188–2197.
37. Bullard, D. C., X. Hu, T. R. Schoeb, R. C. Axtell, C. Raman, and S. R. Barnum. 2005. Critical requirement of CD11b (Mac-1) on T cells and accessory cells for development of experimental autoimmune encephalomyelitis. *J. Immunol.* 175: 6327–6333.
38. Andrades, M. É., A. Morina, S. Spasić, and I. Spasojević. 2011. Bench-to-bedside review: sepsis - from the redox point of view. *Crit. Care* 15: 230.
39. Khasnavis, S., A. Jana, A. Roy, M. Mazumder, B. Bhushan, T. Wood, S. Ghosh, R. Watson, and K. Pahan. 2012. Suppression of nuclear factor-κB activation and inflammation in microglia by physically modified saline. *J. Biol. Chem.* 287: 29529–29542.
40. Wilms, H., J. Sievers, U. Rickert, M. Rostami-Yazdi, U. Mrowietz, and R. Lucius. 2010. Dimethylfumarate inhibits microglial and astrocytic inflammation by suppressing the synthesis of nitric oxide, IL-1beta, TNF-alpha and IL-6 in an in-vitro model of brain inflammation. *J. Neuroinflammation* 7: 30.
41. Bonetti, B., C. Stegagno, B. Cannella, N. Rizzuto, G. Moretto, and C. S. Raine. 1999. Activation of NF-kappaB and c-jun transcription factors in multiple sclerosis lesions. Implications for oligodendrocyte pathology. *Am. J. Pathol.* 155: 1433–1438.
42. Raasch, J., N. Zeller, G. van Loo, D. Merkler, A. Mildner, D. Erny, K. P. Knobeloch, J. R. Bethea, A. Waisman, M. Knust, et al. 2011. IkappaB kinase 2 determines oligodendrocyte loss by non-cell-autonomous activation of NF-kappaB in the central nervous system. *Brain* 134: 1184–1198.
43. Smith, K. J. 2011. Newly lesioned tissue in multiple sclerosis—a role for oxidative damage? *Brain* 134: 1877–1881.
44. Wang, Y., B. Li, Z. Li, S. Huang, J. Wang, and R. Sun. 2013. Improvement of hypoxia-ischemia-induced white matter injury in immature rat brain by ethyl pyruvate. *Neurochem. Res.* 38: 742–752.
45. Wang, Y., P. Yin, S. Huang, J. Wang, and R. Sun. 2013. Ethyl pyruvate protects against lipopolysaccharide-induced white matter injury in the developing rat brain. *Int. J. Dev. Neurosci.* 31: 181–188.
46. Yuan, Y., Z. Su, Y. Pu, X. Liu, J. Chen, F. Zhu, Y. Zhu, H. Zhang, and C. He. 2012. Ethyl pyruvate promotes spinal cord repair by ameliorating the glial microenvironment. *Br. J. Pharmacol.* 166: 749–763.
47. Zeng, J., J. Liu, G. Y. Yang, M. J. Kelly, T. L. James, and L. Litt. 2007. Exogenous ethyl pyruvate versus pyruvate during metabolic recovery after oxidative stress in neonatal rat cerebrocortical slices. *Anesthesiology* 107: 630–640.
48. Bennett-Guerrero, E., M. Swaminathan, A. M. Grigore, G. W. Roach, L. G. Aberle, J. M. Johnston, and M. P. Fink. 2009. A phase II multicenter double-blind placebo-controlled study of ethyl pyruvate in high-risk patients undergoing cardiac surgery with cardiopulmonary bypass. *J. Cardiothorac. Vasc. Anesth.* 23: 324–329.
49. Schuh, C., I. Wimmer, S. Hametner, L. Haider, A. M. Van Dam, R. S. Liblau, K. J. Smith, L. Probert, C. J. Binder, J. Bauer, et al. 2014. Oxidative tissue injury in multiple sclerosis is only partly reflected in experimental disease models. *Acta Neuropathol.* 128: 247–266.